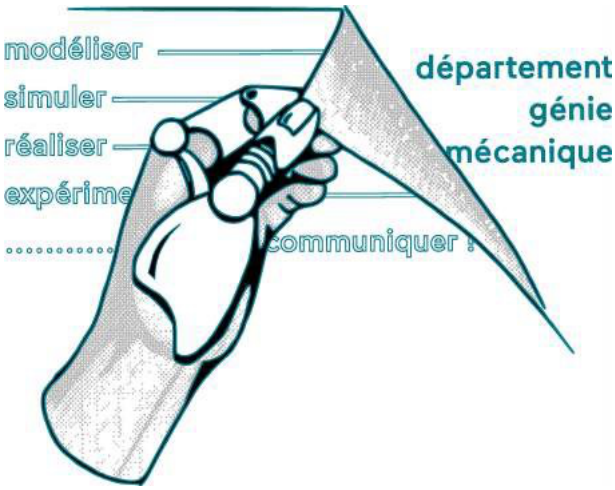

RESEARCH PROJECTS

STUDENTS OF THE DEPARTMENT OF MECHANICAL ENGINEERING

2022-2023

ABSTRACT

Structure of collagen fiber organization in human connective tissues

R. BONNET-EYMARD, M. DIARRA, E. BUDYN

TER M1 2022-2023 Final defence of research projects

école normale supérieure paris-saclay

TER M1 2022-2023
FINAL DEFENCE OF RESEARCH PROJECTS
April 18, 2023, Gif-sur-Yvette, France

Structure of collagen fiber organization in human connective tissues

Romain BONNET-EYMARD*, Mariam DIARRA†, Élisa BUDYN◇

Département de Génie Mécanique
Université Paris-Saclay, École Normale Supérieure Paris-Saclay
4 avenue des Sciences, 91190, Gif-Sur-Yvette
e-mail*: rbonnete@ens-paris-saclay.fr
e-mail†: mariam.diarra@ens-paris-saclay.fr
e-mail◇: elisa.budyn@ens-paris-saclay.fr

KEYWORDS: Bone; Osteocyte process; Collagen fiber; Finite Element Model.

ABSTRACT

General Context

Harvesian bone is a connective tissue with a composite microstructure composed of tubular structures called osteons. The osteons are composed of succesive layers of mineralized collagen fibers of different orientations around the osteon axis. Previous studies [1] showed that fiber orientation is key to understanding the ability of bone to efficiently bear specific loadings. According to J.G. Skedros et al. [2], the black osteons, characterized by fibers oriented at 60/120 degrees, present a better resistance to tensile stress than bright osteons, characterized by fibers oriented at 45/135 degrees, that are subjected to compression loads. To detect their mechanical micro-environment, bone cells exhibit a complex morpholy with numerous cytoplasmic processes that can be imaged and segmented in 3D using fluorescent confocal microscopy [3]. However, the computational cost of the aforementioned methods prevent from developing a numerical model of osteonal lamella microstructure. In that respect, Kamioka et al. [2] developed an homogenized model for the peri-cellular and extra-cellular matrices (PCM, ECM) without explicitly modeling the fibrous microstructure of the bone lamella. Here we present a parameterized 3D collagen fiber model to characterize the mechanical behavior of the bone ECM around an osteocyte process. The Finite Element model explicitly represents the mineralized collagen fibers with accurate orientations, with respect to the centrale axis of a considered osteon, around a representative process of an osteocyte. The study aims at understanding the impact of collagen fiber orientation on the mechanical behavior around resident bone cells.

Methods

To date, the geometry of the osteocyte and its processes were obtained by confocal fluorescence microscopy. The collagen fibers were modeled by parameterized corrugated helices of which the pitch defined the orientation of the fiber around its central axis. To obtain the representative mechanical behavior of the ECM, a representative volume element (RVE) was defined as a cube of 1 μm width containing a segment of a cytoplasmic process of the imaged osteocyte. The RVE was split into two regions, containing each, an ensemble of

collagen fibers with distinct orientations around the osteon axis, denoted $\vec{e_y}$. To generate a set of fiber surface geometries around $\vec{e_y}$, an unique representative fiber part was created, replicated and translated along $\vec{e_x}$ and $\vec{e_z}$ axis until filling completely the RVE with respecting the measured spacing between fibers. Then, the geometry files of the different parts were generated in MatLab, meshed, and implemented in the Abaqus software.

Prospects

The different parts were assembled/substracted to obtain the RVE. Next steps will involve the identification and the implementation of the boundary conditions and constraints between the different parts of the model. The model will simulate the RVE under a strain field, representative of the loading induced by walking. Thus, the mechanical microenvironment of bone cells and the homogenized stiffness tensor of the modeled microstructure will be calculated. The Young's moduli will be compared to previous experimental results. Finally, the two RVEs, respectively representing a bright and dark osteon, will make it possible to compare the tissue mechanical behavior under either tensile or compression stress that are detected by the osteocyte.

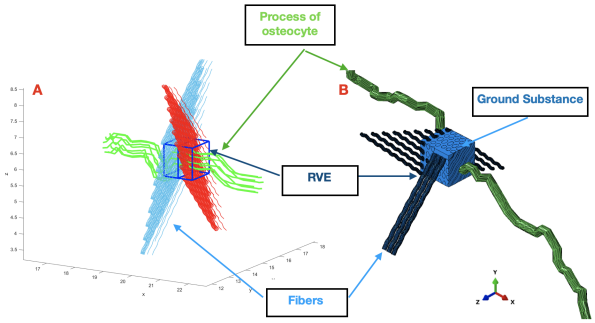

Figure 1: Matlab (A) and Abaqus (B) models of the collagen fibers oriented at 45/135 degrees crossing a process. For clarity, not all fibers are ploted.

REFERENCES

[1] J.G. Skedros, K.E. Keenan, T.J. Williams, C.J. Kiser. Secondary osteon size and collagen/lamellar organization ("osteon morphotypes")are not coupled, but potentially adapt independently for local strain mode or magnitude. Journal of Structural Biology, 2012.

[2] H. Kamioka,Y. Kameo, Y. Imai, A.D. Bakker, R.G. Bacabac, N. Yamada, A. Takaoka, T. Yamashiro, T. Adachif and J. Klein-Nulend. Microscale fluid flow analysis in a human osteocyte canaliculus using a realistic high-resolution image-based three-dimensional model. Integr. Biol., 2012, 4, 1198–1206

[3] E. Budyn, N. Gaci, S. Sanders, M. Bensidhoum, E. Schmidt,B. Cinquin,P. Tauch,H. Petite. Human Stem Cells Derived Osteocytes in Bone-on-Chip. MRS Advances, vol.3(36),P.1143-1455, 2018.

Development and validation of algorithms to generate trajectories for the hybridization of 3D printing processes and machining

T. LE MOIGNE, L. TESSIER, C. TOURNIER

TER M1 2022-2023
Final defence of research projects

école normale supérieure paris-saclay

TER M1 2022-2023
FINAL DEFENCE OF RESEARCH PROJECTS
April 18, 2023, Gif-sur-Yvette, France

Development and validation of algorithms to generate trajectories for the hybridization of 3D printing processes and machining

Théo Le Moigne*, Léo Tessier*, Christophe Tournier†

* Département Génie Mécanique
ENS Paris-Saclay
4 avenue des Sciences, 91190 Gif-sur-Yvette, France
e-mail: {theo.le_moigne,leo.tessier}@ens-paris-saclay.fr

† LURPA — Département Génie Mécanique
ENS Paris-Saclay
4 avenue des Sciences, 91190 Gif-sur-Yvette, France
e-mail: christophe.tournier@ens-paris-saclay.fr

KEYWORDS: machining; additive manufacturing; fused deposition modeling; hybridization; contouring algorithms.

ABSTRACT

Introduction

From the democratization of fused deposition modeling (FDM) in 2009, individuals are as able as manufacturers to use 3D printing thanks to algorithms that convert STL files into G-code that can be directly interpreted by the printer. Nowadays tool changing machines make it possible to rework printed parts with milling cutters to improve their surface quality. The purpose of this study is to develop an algorithm allowing to convert an stl file into a hybrid G-code file generating additive manufacturing and machining trajectories. This algorithm is implemented as a plugin in the open source Cura environment.

Methods

Contouring path calculation algorithms have come a long way with the primary purpose of generating pocket milling paths. First of all, Persson [1] proposed to intersect successive face offsets on the contour skeleton. Then Held [2] developed his "conventional offsets" algorithm in which each face is offset along its normal. The offset edges must then be intersected. The issues raised by this last point are solved by Chuang [3] who extends the method to complex geometries. Finally, Jousselin [4] put forward an intersection algorithm for the contouring problem specifically. Our solution is developed on this basis.

In this first proof-of-concept, one will deal with the case of a single continuous contour with no bottleneck. The points of the given contour are first offset along the normal of the two faces they are belonging to. Then the resulting point cloud is simplified by suppressing all bi-points whose elements are too close according to the norm 2. Then resulting offset faces are intersected. There intersection points are finally kept as edges of the offset contour and are used to build the corresponding edges. Finally, this offset contour is translated

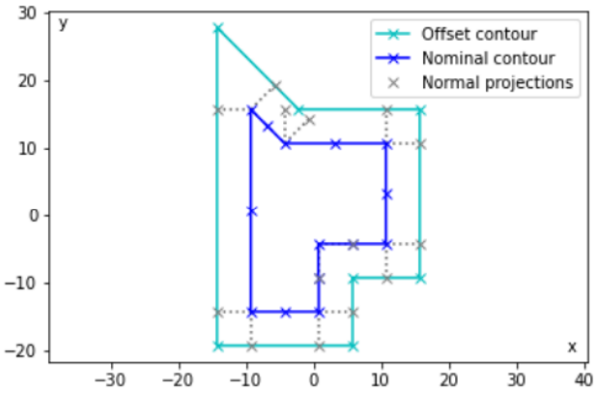

Figure 1: Contouring algorithm result on a layer

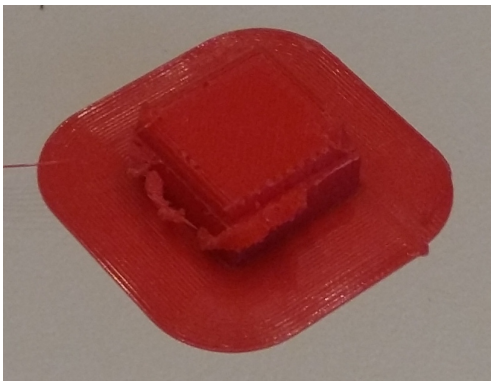

Figure 2: Printed and machined part

as a G-code milling trajectory and add into the additive manufacturing G-code generated by Cura. The final program is executed on the printer in order to be checked.

Key results

First, Python returns satisfying results for a single layer (figure 1) and according to the Cimco G-code simulator, the generation of hybrid tool paths on the whole part can also be validated. Nonetheless when it comes to real tests on the printer (figure 2), the plastic has to be over extruded to compensate for inaccuracies and ensure the contact between the part and the cutter. Moreover, due to the lack of machine references, tool gauges can hardly be measured in the machine, resulting in positional error in the range of 0.1mm.

Concluding remarks

Thus the hybridization algorithm is validated in this simple case. Further studies could be carried out on the algorithm to make it robust to more complex geometries such as cylinders, bottlenecks or spikes. Furthermore, the tool gauge measurement process needs to be improved using CMM technologies for example. Finally, an experimental study could be led to choose the proper material, tools and milling conditions.

REFERENCES

[1] H. Persson. NC machining of arbitrarily shaped pockets. *Computer-Aided Design* **10**:169-174, 1978.

[2] L. Andor, M. Held, G. Lukacs. Pocket machining based on contour-parallel tool paths generated by means of proximity maps. *Computer-aided design* **26**:189–203, 1994.

[3] CM. Chuang, HT. Yau. A new approach to z-level contour machining of triangulated surface models using fillet endmills. *Computer-Aided Design* **37**:1039-1051, 2004.

[4] B. Jousselin. *Développement d'une méthodologie de génération de trajectoires d'ébauche en usinage 5 axes*, Université Paris-Saclay, 2020.

Experimental study of the buckling of metamaterials under bicompression ANR Max-Oasis

J. Bourgain-Wilbal, C. Rey, M. Poncelet, C. Combescure

TER M1 2022-2023
Final defence of research projects

école normale supérieure paris–saclay

TER M1 2022-2023
FINAL DEFENCE OF RESEARCH PROJECTS
April 18, 2023, Gif-sur-Yvette, France

Experimental study of the buckling of metamaterials under bicompression ANR Max-Oasis

Julien Bourgain-Wilbal [*], **Clément Rey** [*],
Martin Poncelet [†], **Christelle Combescure** [◇]

[*] Mechanical Engineering Department
École Normale Supérieure Paris-Saclay
e-mail: julien.bourgain–wilbal@ens-paris-saclay.fr clement.rey@ens-paris-saclay.fr

[†] Laboratoire de Mécanique Paris-Saclay
Université Paris-Saclay / CentraleSupélec / ENS Paris-Saclay / CNRS
e-mail: martin.poncelet@ens-paris-saclay.fr

[◇] IRDL
UBS/ENSTA-Bretagne/ENIB/UBO / CNRS
e-mail: c.combescure@st-cyr.terre-net.defense.gouv.fr

KEYWORDS: Metamaterials; Bicompression; Buckling; Simulation ; Conception.

ABSTRACT

Context and introduction

Cellular honeycomb materials are increasingly used for their very favorable strength to mass ratio compared to bulk materials. However, the buckling behaviour of such materials is yet to be understood. Our project aims at experimentally validate a numerical approach to model this behaviour, developed by C. Combescure et al. [1], via designing a bicompression testing machine. Other researchers also worked on such machines [2] [3] [4], yet their machines could only measure normal forces which are not sufficient to define boundary conditions. This paper focuses on designing an enhanced testing machine to measure torques and normal and tangential forces applied to the sample, constructing such sample and simulating its behaviour with a finite elements code.

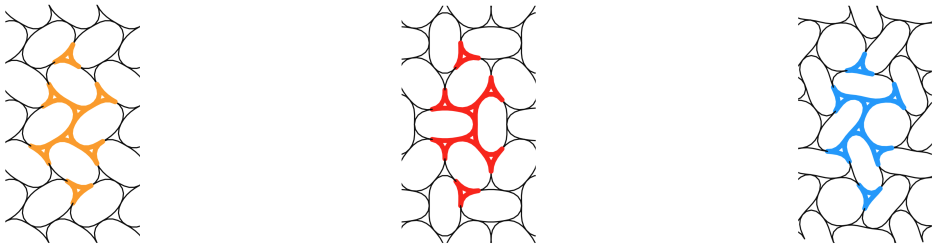

(a) Cod (b) Butterfly (c) Flower

Figure 1: Buckling patterns observed on a cellular honeycomb sample under bicompression [1]

Methods

To decide on which machine to base ours, the main criteria are the uniformity of the normal stress and the least tangential effort. Two approaches were made. The first one was based on freehand calculations using strong hypotheses, which led to indeterminacy with Shan machine. The second one was to simulate the variation of the normal and tangential stresses in the sample using FEM, considering the different mechanisms.

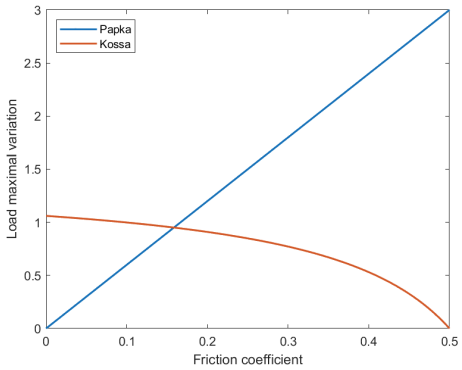

Figure 2: Analytic calculation of the variation of the normal loading along a surface

Creating and manufacturing the sample are not to be neglected. The choice of a material allowing elastic and non viscous great deformations converges toward silicon. After several tests, samples are made in silicon poured in a 3D-printed PLA mold, and designed thick to prevent out-of-plane buckling which would deteriorate the measure of in-plane buckling. The machine is then made in wood, which can be considered rigid with respect to silicon.

Results and Interpretation

The simulation using finite elements tends to show the best machine among the 3 reviewed machines was designed by S.D. Papka. In fact, for a friction coefficient lower than 0.15, this design seems to impose the least tangential stress and the most uniform normal stress. A more in-depth study is on its way.

REFERENCES

[1] C. Combescure, R.S. Elliott, N. Triantafyllidis. Deformation patterns and their stability in finitely strained circular cell honeycombs. *J Mech Phys Solids* **142**:Pages, 2020.

[2] S.D. Papka, S. Kyriakides. Biaxial crushing of honeycombs - Part I : Experiments. *Int J Solids Struct* **36**:4367-4396, 1999.

[3] S. Shan et al. Harnessing Multiple Folding Mechanisms in Soft Periodic Structures for Tunable Control of Elastic Waves. *Adv Funct Mater* **88**:296-318, 2016.

[4] A. Kossa. A new biaxial compression fixture for polymeric foams. *Polym Test* **45**:47-51, 2015.

Numerical modelling of woven fabrics subject to stabbing

L. Jammes , S. Cochard, C. Ha Minh

TER M1 2022-2023
Final defence of research projects

école normale supérieure paris–saclay

Numerical modelling of woven fabrics subject to stabbing

L. Jammes*, S. Cochard†, C. HA Minh ◇

*† Mechanical engineering
École Normale Supérieure Paris-Saclay
4 Av. des sciences, Gif-sur-Yvette, 91190

* e-mail: louka.jammes@ens-paris-saclay.fr

† e-mail: salome.cochard@ens-paris-saclay.fr

◇ Laboratoire de mécanique de Paris-Saclay
École Normale Supérieure Paris-Saclay
4 Av. des sciences, Gif-sur-Yvette, 91190
e-mail: cuong.ha-minh@ens-paris-saclay.fr

KEYWORDS: Woven fabrics; Stabbing; numerical modelling.

ABSTRACT

General Context

Personal protection against stabbing is developing continuously to meet a growing need. Indeed, while the regulations on firearms are becoming more and more severe, knife attacks represents still a persistent and worrying concern for the well-being of society. Thus, the development of high-performance anti-stabbing vests is becoming a priority. To produce such protections, the study of flexible woven fabrics, and new technological answers associated, such as shear-thickening fluids, are key. Until now, there has been many numerical and experimental studies on the behavior of woven fabrics submitted to ballistic impact[2]. However, the ones addressing stabbing impacts remain mainly experimental; and the few ones offering analytical models [3], or numerical simulations[4], of the woven fabrics behavior apply mostly for static impact, are not conducted under the NIJ 0115 regulation [1], a document stating the standards body armors have to meet in term of stab resistance. This is why this study aims to meet this standard by predicting the behavior of woven fabrics subject to the same dynamic loads as in this norm. We will put in perspective two numerical models to compare their results and conclude on the accuracy of a numerical approach compared to an experimental approach.

Matlab Simulation

Most models currently available are designed to study ballistic impacts, but during stabbing the speeds involved are much lower, making the mechanisms of dissipation of energy potentially different, which we will study here. During a ballistic impact the energy of the impactor is dissipated through the deformation of the fabric, the transmission of momentum to a pyramid of fabric, and through friction [2]. We coded an iterative model on Matlab using these principles. The speed of the impactor is updated at each iteration with the principle of energy conservation. The results obtained regarding the evolution of kinetic and deformation energies during a simulation 2 only showed a 10% difference with experimental results [2] and a 14 % error in the evolution of the pyramid's height and width. For the rest of the project we will aim to validate the use of this model with lower speeds and compare its results with a finite element analysis.

Radioss Simulation

To begin with, in order to understand the phenomenons on a microscopic level, we only simulated the interaction between the knife and a single fibre. The input material chosen for the knife is steel, and the

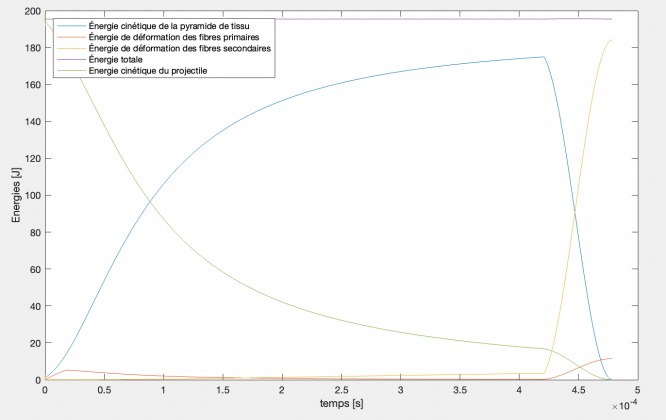

Figure 1: Evolution of kinetic and deformation energies during a simulation .

one for the fiber is Kevlar KM2. The knife has been given an imposed velocity, while the ends of the fibre are fixed. As in the Matlab model, we can see that the impact of the knife on the fiber creates a wave of deformation and stress, that spread throughout the entire fibre (figure 2). We will then simulate the behavior of 3 fibres, which implies to understand the nature of the interaction between the different fibers. Finally, we will eventually simulate the interaction of the knife with an entire string, which is composed of a about twenty fibers.

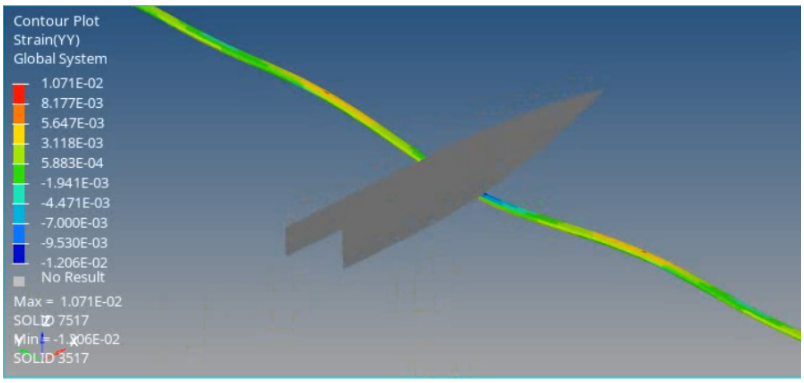

Figure 2: Wave of deformation in the fiber simulated on Radioss

REFERENCES

[1] Julie E. Samuels, *Stab Resistance of Personal Body Armor NIJ Standard–0115.00*. U.S. Department of Justice, September 2000.

[2] Cuong Ha-Minh, Abdellatif Imad, François Boussu, Toufik Kanit. On analytical modelling to predict of the ballistic impact behaviour of textile multi-layer woven fabric. *Composite structures* **Vol 99**: Pages 462–476, Year 2013.

[3] Limin Hou, Baozhong Sun, Bohong Sun. An analytical model for predicting stab resistance of flexible woven composites. *Springer*, Year 2012.

[4] Cuong Ha-Minh, Benjamin Provost, François Boussu, Daniel Coutellier, Abdellatif Imad. Vers la géométrie réelle d'un tissu 3D interlock sur la précision de la simulation numérique à l'impact. *HAL*, Year 2018.

Study of strategies and geometric parameters in repair by wire deposition

E. RUIZ, C.HEITZ, Y.QUINSAT, N.MULLER

TER M1 2022-2023
Final defence of research projects

école normale supérieure paris–saclay

Study of strategies and geometric parameters in repair by wire deposition

Elisabeth RUIZ[◇], Clément HEITZ[◇], Yann QUINSAT[*], Nicolas MULLER[*]

[◇] DGM
ENS Paris-Saclay
4 Avenue des Sciences, 91190 Gif-sur-Yvette,
e-mail: clement.heitz@ens-saclay.fr ,
elisabeth.ruiz@ens-paris-saclay.fr

[*] Lurpa
ENS Paris-Saclay
4 Avenue des Sciences, 91190 Gif-sur-Yvette
e-mail: yann.quinsat@ens-paris-saclay.fr,
nicolas.muller@ens-paris-saclay.fr

KEYWORDS: WLAM; Welding; additive manufacturing; 316L; mechanical repair

ABSTRACT

General context

WLAM (Wire-Laser Additive Manufacturing) is a recent subject on which only few researchers have investigated. This new technology allows building volumetric objects composed of different layers of welded metal. The aim of our research is to examine the manageability of reusing metal mechanical parts that have been damaged in surface. Indeed, WLAM offers an interesting way of reusing defective high-valued pieces. Instead of destroying the parts, they are machining to remove the defect and the possible contaminants. The missing parts are then recreated by depositing successive layers of materials.

Few previous researches have been carried out about the mechanical properties, microstructures, corrosion resistance and stress corrosion performance of the 316L stainless steel using WLAM. Nevertheless, none of them have studied which parameters and strategies of filling seem to be the best to repair pitting corrosion defects.

In our study, we focused on finding the optimized parameters and strategies to repair 316L stainless steel parts ruined by corrosion pitting, using WLAM. It is the continuity of a previous research carried out by the laboratory LURPA about finding the optimized form of the pitting corrosion in a 316L stainless steel part using Laser Metal Deposition (LMD) [1].

Methods

Finding the parameters to optimize the deposit of metals can only be done empirically at first. We based our initial parameters values on those given in two particular papers [2][3]. The main parameters that define the welding strategy are the wire feed speed, the nozzle travel speed and the laser power. For a volumetric construction, we also define the coverage rate between the beads and the layer height. We established 3 test campaigns in order to determine the parameters separately. In a first time, we focused on finding which set returns the best weld bead continuity. Then, we studied which coverage rate gives at the same time the best overlap between beads and the lowest internal porosity.

(a) Hybrid robot cell of the Lurpa *(lurpa.ens-paris-saclay.fr)*

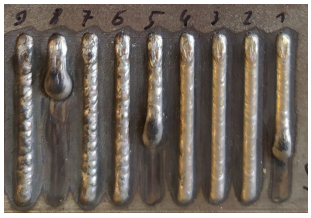

(b) First campaign: single beads

(c) Second campaign: bead rugs

Figure 1

The aim of the first campaign was to find the optimized wire feed speed when fixing the laser power and the nozzle travel speed. It consisted in making simple beads (figure 1b) with the Lurpa's hybrid robot cell (figure 1a) with different values of wire feed speed and then comparing their continuity and their dimensions.

The second campaign allowed us to fix a satisfying coverage rate between two beads. We realized 3 bead rugs, each with a different rate: 40%, 50% and 60% (figure 1c). To identify the best, we noted if there were swelling of the beads, jumps or other defects. Moreover, we took time to analyze the microstructure of polished sections of each rug in order to see the porosities. We also compared the differences of microhardness between the beads and the substrate.

Finally, the last campaign is planned to evaluate the impact of the volume geometry and choose the best filling pattern between zig-zag and outlines. Flat-bottomed pyramid pockets with 3 different angles of attack have been machined. They will be filled using WLAM by following the two strategies. However, we have difficulties to define the trajectories for the outline method : the width of the bead is almost as large as the width of the volume to fill. Therefore, we cannot fill exactly the volume with a constant bead width.

Key results and conclusion

From the 2 first campaigns, we identified an adapted set of parameters to weld rugs of stainless steel 316L with WLAM. The optimal wire speed is 2.3mm/min for a power of 2750W and a feed rate of 0.19mm/min. The bead is then approximately 1.4mm in height and 3.3mm in width. The coverage rate with the fewest jump, swelling and porosity defects is that of 40%.

We also determined that it is more suitable to use a zig-zag pattern to fill a volume that is smaller than the bead's width. At the moment, it is the only strategy we can use properly but a strategy with a lead width adaptation would be very interesting. Further studies are also needed in order to validate the welding parameters with other geometries and try different filling strategies.

REFERENCES

[1] B.Si Smail. *Integrated approach to 316L stainless steel parts repair for pitting corrosion using Laser Metal Depositione*. 2022.

[2] T.Feldhausen. *Mechanical Properties and Microstructure of 316L Stainless Steel Produced by Hybrid Manufacturing*. 2020.

[3] M.Bassis. *The Effect of a Slow Strain Rate on the Stress Corrosion Resistance of Austenitic Stainless Steel Produced by the Wire Laser Additive Manufacturing Process*. 2021.

Monitoring of the wire-laser additive manufacturing process (WLAM) using a confocal thermal camera

R. MANNARELLI, A. TISSANDIER, K. GODINEAU, N. MULLER.

TER M1 2022-2023
Final defence of research projects

école normale supérieure paris–saclay

TER M1 2022-2023
FINAL DEFENCE OF RESEARCH PROJECTS
March 15, 2023, Gif-sur-Yvette, France

Monitoring of the wire-laser additive manufacturing process (WLAM) using a confocal thermal camera

Rafael MANNARELLI[1], Alexandre TISSANDIER[1], Kevin GODINEAU[2], Nicolas MULLER[2]

[1] Université Paris-Saclay, ENS Paris-Saclay, Mechanical Engineering Department, Gif-sur-Yvette 91190 e-mail: rafael.mannarelli@ens-paris-saclay.fr, alexandre.tissandier@ens-paris-saclay.fr

[2] Université Paris-Saclay, ENS Paris-Saclay, LURPA, Gif-sur-Yvette 91190
e-mail: kevin.godineau@ens-paris-saclay.fr, nicolas.muller@ens-paris-saclay.fr

KEYWORDS: Additive Manufacturing, Monitoring *in-situ*, Data analysis

ABSTRACT

General Context

Additive manufacturing is a class of processes consisting of adding material to a substract, usually layer by layer, to make 3D objects from a model. The Wire Additive Manufacturing (WXAM) combines Wire Arc Additive Manufacturing (WAAM) and Wire Laser Additive Manufacturing (WLAM) processes to create 3D objects by melting a metal wire that is further deposited on a substrate. Offering higher deposition rates than powder bed processes, it does not raise the hygiene, safety, and environmental issues associated with the latter [1], while allowing the creation of complex shapes.

To date, WAAM technique have been well studied since this process derives from conventionnal welding [2]. In contrast, research on WLAM has mostly focused on investigating the control of transfer mode effects and phenomenon at a granular scale [3], while the monitoring of this process has been overlooked. Moreover, using a laser allows a better control of energy deposition compared to the arc. In this context, this project aims to contribute to the development of the WLAM technique by producing a proper monitoring system and understanding the defaults' origins. By integrating information such as temperature mapping and advance speed, feed rate and laser power, it should provide a better understanding of the physical phenomena underlying the WLAM production process. Thus, this model should allow more effective control of this process.

Methods

Our system comprises a printhead mounted on a 6-axis robot, with 3 laser beams focusing on the metal wire to melt it. In addition, the laser system is fitted with a confocal thermal camera. Data synchronization from this camera and processing of internal sensors will be used to create a volumetric model of the produced part. Thus, data extraction occurs in two parts. Relevant information is selected, and a sequence of trajectories have been made up and implemented to generate data. The data is standardized into MatLab tables and synchronized temporally. Linear and nearest-neighbor time-interpolation is utilized to fill in missing data. The correlation between information is analyzed graphically.

Results

We were able to extract and analyze all of our parameters, namely position, velocity, acceleration, laser power, wire exit velocity, laser activation, maximal temperature and area. An example of the results on the impact of velocity on welding beads can be found below.

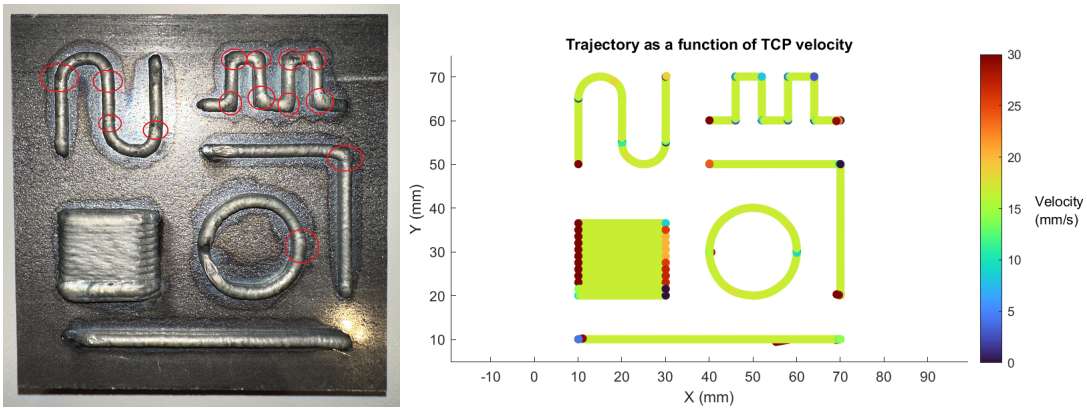

Figure 1: Comparison between traced datas and the welded part

The red areas marked in the photo above represent clusters resulting from the decrease in velocity that we observed in the display of trajectories as a function of speed. We were also able to deduce that when velocity increases, the opposite effect occurs, and matter is stretched, resulting in thinner beads.

Further work

Up until now, we have made many observations but it would be interesting to properly characterize the camera in order to make sense of the extracted data and be able to use it. Indeed, the thermal camera's focal range passes through the three lasers path, If the mean of the results derived from image analysis is not understood, it becomes irrelevant and pointless. Moreover, in order to minimize errors associated with process defects, it would be wise to categorize these defects based on the various parameters that we have identified, and then implement corrective measures.

References

[1] Donghong Ding et al. "Wire-feed additive manufacturing of metal components: technologies, developments and future interests". eng. In: *International journal of advanced manufacturing technology* 81.1-4 (2015), pp. 465–481.

[2] Shangyong Tang, Guilan Wang, and Haiou Zhang. "In situ 3D monitoring and control of geometric signatures in wire and arc additive manufacturing". In: *Surface Topography: Metrology and Properties* 7.2 (May 2019), p. 025013.

[3] M. Mortello and G. Casalino. "Transfer mode effects on Ti6Al4V wall building in wire laser additive manufacturing". In: *Manufacturing Letters* 28 (2021), pp. 17–20.

Ultrasonic reflection matrices separation in simple and multiple scattering subspaces by using deep learning

E. Largeteau, A. Corduant, N. Belkhir, C. Brütt, F. Feyel

TER M1 2022-2023
Final defence of research projects

école normale supérieure paris–saclay

TER M1 2022-2023
FINAL DEFENCE OF RESEARCH PROJECTS
April 18, 2023, Gif-sur-Yvette, France

Ultrasonic reflection matrices separation in simple and multiple scattering subspaces by using deep learning

E. Largeteau*, A. Corduant*, N. Belkhir†, C. Brütt†, F. Feyel◇

* ◇ Département de Génie Mécanique
École Normale Supérieure Paris-Saclay
4 avenue des Sciences, 91190 Gif-sur-Yvette, France
* e-mail: etienne.largeteau@ens-paris-saclay.fr and antoine.corduant@ens-paris-saclay.fr
◇ e-mail: frederic.feyel@ens-paris-saclay.fr

† Safran Tech
Rue des jeunes Bois, 78117 Châteaufort, France
e-mail: nacim.belkhir@safrangroup.com and cecile.brutt@safrangroup.com

KEYWORDS: Ultrasonic reflection matrices; Deep Learning ; Autoencoders.

ABSTRACT

General context

Nondestructive testing is an essential aspect of modern-day engineering. Its purpose is to verify the structural integrity of a critical piece without altering its characteristics in any way. This method is achieved through the use of ultrasound, which is widely utilised due to its cost-effectiveness and simplicity. However, some difficulties may arise when working with highly polycrystalline materials, such as certain titanium alloys. The non-destructive testing process involves emitting ultrasonic waves through the piece using an array of transducers and capturing the echoes with the same array. By doing so, a reflection matrix (Figure 1) can be created, which contains the responses of each transducer at a given frequency of each transmitted signal. The echoes originate from scatterers in the material, which may be defects or crystals oriented in various directions. In some cases, certain materials such as titanium alloys may have such a high concentration of natural strong scatterers that a defect can be concealed. This is due to the phenomenon of multiple scattering, where a wave can "bounce" on multiple scatterers before returning to the array. To obtain a clear image of the piece, a mathematical correction can be applied to remove the multiple scattering from the reflection matrix and generate a single scattering matrix. However, this correction is nearly impractical under real-world conditions.

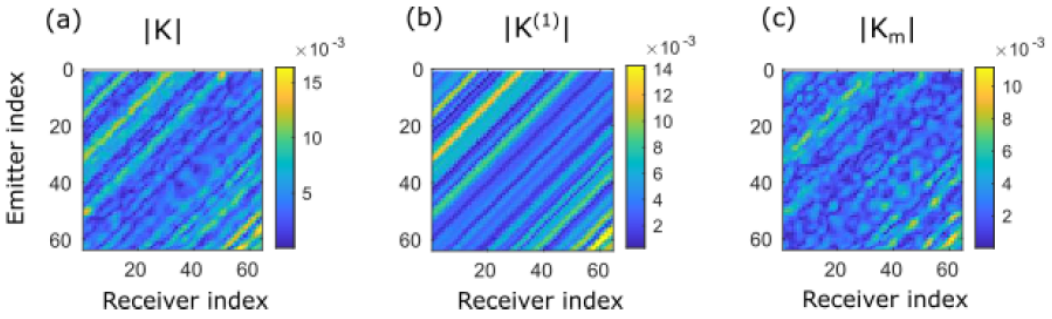

Figure 1: Total, single and multiple scattering matrix

Preliminary research

We studied the influence of the autoencoder's parameters such as the learning rate, the batch size and the dimension of the latent space on other kinds of data to optimise our results and understand in depth the subject. The datasets studied were MNIST [3] (pictures of handwritten digits) and MNIST-audio [1] (audio recording of spoken digits). The results of the reconstruction of MNIST images with an autoencoder are presented Figure 2a. On MNIST-audio, the autoencoder has been applied to the spectrogram of the sound signal only, because of the similarity between it and the reflection matrices and also because of the promising results obtained for classifying the signal (determining the number said in the audio). Convolutional layers have been used for all these tasks and will be used for the final model.

Our project

In order to overcome the scattering effect of the polycrystalline structure we chose to use a deep learning approach by training an autoencoder to reconstruct a single scattering matrix from a total scattering matrix. We used the numerical simulation code written by C.Brutt [2] to generate the training data. This code uses wave theory to find, for a random dispersion of scatterers, all the scattering matrices and in particular the single and total scattering matrix. The information created by the reflection can be used in different forms. We can use the raw temporal signal, but this is taking a lot of memory. The second form of input is the Fourier transform of this temporal signal. The last form is creating a spectrogram from the temporal signal (caught in between the two last approaches). We already have some results on applying autoencoders for the separation of reflection matrices, presented in 2b, but further research is needed.

(a) MNIST results with latent space of dimension 8 (b) Reflection matrix results

Figure 2: Results from an autoencodeur

References

[1] Sören Becker **andothers**. "Interpreting and Explaining Deep Neural Networks for Classification of Audio Signals". **in***CoRR*: abs/1807.03418 (2018). arXiv: 1807.03418. URL: http://arxiv.org/abs/1807.03418.

[2] Cécile Brütt **andothers**. "Weight of single and recurrent scattering in the reflection matrix of complex media". **in***Phys. Rev. E*: 106 (2 **august** 2022), **page** 025001. DOI: 10.1103/PhysRevE.106.025001. URL: https://link.aps.org/doi/10.1103/PhysRevE.106.025001.

[3] Y. LeCun **andothers**. "Gradient-Based Learning Applied to Document Recognition". **in***Proceedings of the IEEE*: 86.11 (**november** 1998), **pages** 2278–2324.

Analysis of thermomechanical properties of NiTi alloys under bi-axial charges

A. Dallot , M. Thiriet , B. Durand

TER M1 2022-2023
Final defence of research projects

école normale supérieure paris–saclay

Analysis of thermomechanical properties of NiTi alloys under bi-axial charges

A. Dallot [*], M. Thiriet [*], B. Durand [◇]

Ecole normale supérieure Paris-Saclay
4 Avenue des Sciences, 91190 Gif-sur-Yvette, France
[*] Department of Mechanical Engineering
e-mail :{alexendre.dallot,martin.thiriet}@ens-paris-saclay.fr
[◇]LMPS - Laboratoire de Mécanique Paris-Saclay
e-mail : bastien.durand@ens-paris-saclay.fr

Keywords : Bi-axial compression ; Nickel ; Titanium ; chocs ; wave theory ; thermomechanics

Abstract

General Context

When it comes to violent chocs and perturbations in solids, high velocity bi-axial stresses are quite common. High velocity chocs require a particular study as it implies thermomechanical behaviors. For simple material like pure aluminum, elastic deformations due to temperature may be neglected in comparison to plastic deformations due to the choc. For over material such as Nickel-Titanium alloys, mechanical behaviors are heavily impacted by heat perturbations. Indeed, changes in the crystalline structures of the alloy cause plastic deformations to produce significant temperature gains. Thus, thermal deformations cannot be neglected anymore.

The main purpose of this study is to characterize the mechanical behavior of Nickel-Titanium alloys with a Bi-axial Hopkinson bar experimental platform, in order to confront the platform of K.Jin and al [1] which produces the mechanical load with electromagnetic hammers.

Methods

To produce a 2D stress load a complex rig is need. A single axis Hopkinson bar setup can be used to do multi axial compression [2], but in order to make multi-axial loads easier to experiment with, a dedicated setup is built. The 3D rig sends a projectile towards a load converter that spreads the load in 4 rods equally. The shock wave is then redirected toward the sample. 8 strain gauges allows us to monitor the propagation of the shock wave.

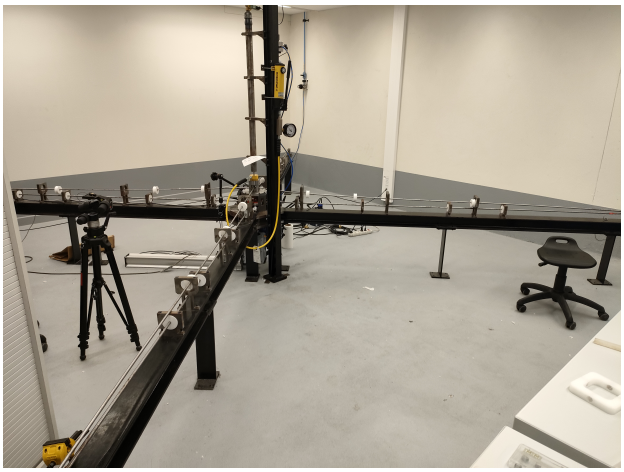

FIGURE 1 – 2D hopkinson bar setup

To make sure that the strain gauges do not give faulty results, a high speed camera is used to record the sample being crushed. Image correlation is then used on those high speed images to obtain the strain field in the sample. Then the movement of the end of the sample can be deduced and confirm the data provided by the strain gauges.

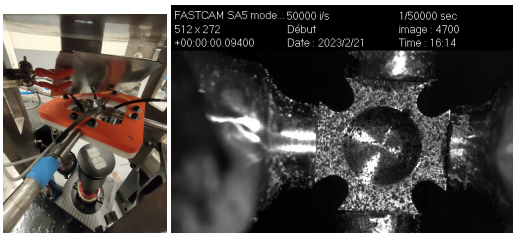

FIGURE 2 – 2D hopkinson bar setup high speed camera

Once the 2D characteristics of the material have been deduced, they can be verified by testing known material, and by using computer simulation to validate that, the material acts the same in the simulation and while testing.

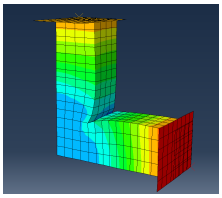

FIGURE 3 – Abaqus simulation of the crushed sample

If the setup is proven to work well on known material, new materials like Ni-Ti can be tested to find their properties. To further extend the possibilities of the rig, a high speed thermal camera is also used to measure the temperature of the sample while it is being hit. The temperature of the sample can be especially useful for some allows like Ni-Ti.

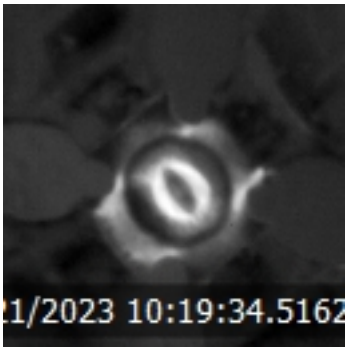

FIGURE 4 – Thermal image of the sample under bi-axial compression

Results

With the first tests, we were able to confirm that the setup is able to deliver results that are similar to what simulations are able to deliver on known material like aluminum. This means that further researches can be done with different materials that are not yet fully characterized.

REFERENCES

[1] K.Jin and al, A novel technique to measure the bi axial properties of materials at high strain rates by electromagnetic Hopkinson bar system. *ELSEVIER, International Journal of Impact Engineering*, 2022.

[2] : B. Durand, P. Quillery, A. Zouari, H. Zhao Eploratory Tests on a Biaxial Compression Hopkinson Bar Set-up. *AL open science. Experimental Mechanics, Society for Experimental Mechanics*, 2020.

[3] : J.Mohd Jani, M.Leary, A.Subic, M. A.Gibson. A review of shape memory alloy research, applications and opportunities. *Elsevier, Materials and Design*, 2013.

Experimental characterization of added mass force in dry granular matter

L. Grasset , T. Perrot , B. Darbois-Texier , A. Seguin , P. Gondret

TER M1 2022-2023
Final defence of research projects

école normale supérieure paris—saclay

TER M1 2022-2023
FINAL DEFENCE OF RESEARCH PROJECTS
April 18, 2023, Gif-sur-Yvette, France

Experimental characterization of added mass force in dry granular matter

L. Grasset*, T. Perrot*, B. Darbois-Texier◇, A. Seguin◇, P. Gondret◇

* Mechanical Engineering Department, ENS Paris-Saclay, 91190 Gif-Sur-Yvette, France

◇ Université Paris-Saclay, CNRS, FAST, 91405 Orsay, France

KEYWORDS: Added-mass force ; Dry granular matter ; Fluid dynamics ; Non-Newtonian fluids ; Experimental characterization.

ABSTRACT

Background The problem of a solid body moving in a fluid is a textbook case in fluid mechanics and has many industrial applications. During a rectilineal motion at a constant speed, the action of the fluid on the solid is described as the drag force, only due to the viscosity of the fluid. Considering an unsteady movement, an extra contribution to this force appears : it is the added-mass force F_{AM} which depends linearly of the acceleration $a(t)$ of the body scaled with the added mass coefficient C_{AM} and with the mass of fluid displaced ρV ($F_{AM} = \rho V C_{AM} a(t)$) [1]. Furthermore, this coefficient C_{AM} is determined by the geometry of the solid body and by the rheologic properties of the medium.

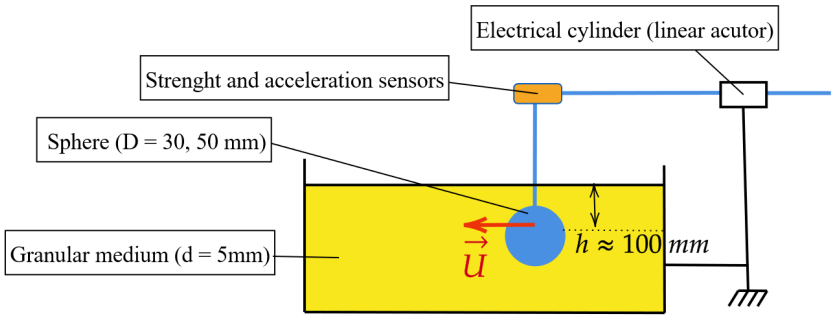

Figure 1: Scheme of the experimental setup

Project definition However, this phenomenon remains unexplored in a dry granular medium (which consists in a set of small solid particles that behave at a macroscopic scale as a non-newtonian fluid [2]). A moving solid in a granular medium is classicaly described by the Froude number $Fr = U/(gh)$ (with U the speed of the solid, g the gravitationnal acceleration and h the depth of the solid), which is the equivalent of the Reynolds number for granular media. Unsteady movements have only been simulated numericaly in 2022 as well as the classic steady drag force in a 2D granular medium [3], and it resulted in two main conclusions : (i) The steady drag is independant from velocity at low Froude numbers ($Fr < 1$), (ii) in the unsteady case, the newtonian expression remains the same, but with an added-mass coefficient depending from the ratio between the body's size and

the grain's diameter (d/D). This is where our study takes place : its goal is to wether confirm or infirm the simulated results by an experimental approach.

Experimental method The experiment is made of a sphere immerged in a granular matter pool (dry and single diameter grains), bound by a thin metal bar to an actuator controlled in speed and acceleration, as illustrated on fig. 2. To quantify the effect of the d/D ratio, we immerged two spheres of differnt sizes at an average depth in the same granular material.

We conducted several tests at steady and unsteady speeds, measuring the force applied to the sphere and its acceleration. At each time we begun the motion by a steady slow speed to establish the contact chains in the grains, and then we accelerated at the final velocity or acceleration as in the simulations [3].

First results First, the tests conducted at a constant velocity confirm the independance of the drag to speed for the range of Froude numbers tested (over 2 decades) as visible in the fig.2. Second, the tests at a constant acceleration are expected to characterise the added-mass effect as soon as treated. This final purpose is to develop relevant predictive models describing unsteady motion of solids bodies in granular media to better understand the underlying principles of the physics of grains.

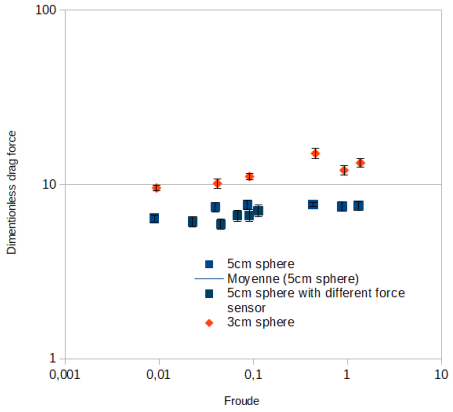

Figure 2: Steady drag force

REFERENCES

[1] C. E. Brennen. *A review of added mass and fluid inertial forces*. DTIC, 1982.

[2] P. Jop, Y. Forterre, O. Pouliquen. *A constitutive law for dense granular flows*. Nature, **441** : 2006

[3] A. Seguin, P. Gondret. *Added-mass force in dry granular matter*. Physical review E **105**: 2022.

Dynamic behavior of optical fiber coils: model validation by mechanical measurements and optical interrogation

E. ALAGOZ, I. THOMAS, F. LOUF

TER M1 2022-2023
Final defence of research projects

école normale supérieure paris-saclay

TER M1 2022-2023
FINAL DEFENCE OF RESEARCH PROJECTS
March 14, 2023, Gif-sur-Yvette, France

Dynamic behavior of optical fiber coils: model validation by mechanical measurements and optical interrogation

Eren ALAGOZ, Ilann THOMAS

Mechanical Engineering Department
Ecole Normale Supérieure Paris-Saclay
4 Avenue des Sciences, 91190 Gif-sur-Yvette
e-mail: eren.alagoz@ens-paris-saclay.fr and ilann.thomas@ens-paris-saclay.fr

Supervised by François Louf (LMPS) and Vincent Crozatier (Thales R&T)

KEYWORDS: homogenization; modal analysis; experimental modal analysis; fiber-optic coil; finite element method.

ABSTRACT

General context

The performance of radar, navigation and communication systems using microwave signals is highly dependent on their reference frequency, which is often imposed by a quartz oscillator. Oscillators must have a precise reference frequency, i.e. low phase noise, and increasing their frequency allows for better system performance, for example by detecting smaller objects. However, the performance of quartz oscillators can be insufficient because they operate at frequencies below a few hundred MHz. Another technology, optoelectronic oscillators (OEO), run at frequencies higher than the GHz. However, a degradation of the phase noise in a severe vibratory environment is then observed, which decreases the performance of the system [3]. This degradation is mainly due to a component of the OEO: the fiber optic coil. Thus, we seek to create and experimentally validate a mechanical numerical coil model allowing us to know its deformations in a vibratory environment in order to eventually compensate for the phase noise of the oscillator.

Modelisation

We decided to move towards a homogenized model of the coil, which avoids fine representation of the structure of the multi-material fiber (silica core and cladding) and the coil, thus facilitating the modeling. The objective of this research project is first to build a mechanical model of fiber optic coil valid in low frequency dynamics, in order to confront it with the results of former numerical models of coils [1] [2]. In his study, I. A. Esipenko focused on the thermoelastic behavior, examining the possibility of switching from a structurally inhomogeneous model of the coil to a transversely isotropic homogeneous medium when calculating the thermal drift of a fiber optic gyroscope [1]. Another study by Ö. Kahveci seeks to characterize the dynamic behavior of an optical fiber coil, by confronting results from a modal experimental analysis (shock hammer) and a finite element model developed with an RVE (figure 1) approach to obtain equivalent material properties The mode shapes and natural frequencies from the experimental modal analysis are then used for the fitting of the FE model [2]. We have thus realized a first FE modeling of coils (Cast3M), exploiting the equivalent material properties of the coil studied by Ö. Kahveci as well as its dimensions. The same modal deformations and eigenfrequency values of the modes were observed, which validated our model. Therefore, it is necessary to characterize the values of the homogenized mechanical parameters of these coils to obtain coherent results for the 4 coils at our disposal. A homogenized numerical model was therefore built (Cast3M), from a RVE based on the structure of our coils (compact hexagonal fibers stacking within the coil). Mechanical properties of the different constituents (glass, acrylate, epoxy resin) were taken from a previous paper [4]. Using the homogenized values, a program computing the first 10 radial/ortho-radial modes has been implemented. To correctly represent the bending modes, parabolic 3D elements are used in the FE model.

Experimentation

An experimental shock hammer vibration study was conducted on two coils of different sizes, using a single axis accelerometer for our measurements. To obtain all the planar (figure 3 & 4) and out-of-plane ovalization eigenmodes, coils are excited and measured radially a 1st time and in its axis on a 2nd. Finally, the measured frequencies of the 3 first out-of-plane modes are respectively 455.6, 1469.4 and 2690 Hz. It is difficult to identify the modes at high frequencies (>3 kHz), because a significant level of damping of the structure occurs then, mainly caused by the coil's matrix. In addition an optical interrogator experiment was conducted. This study consisted in exciting a 1 km fiber coil with a shock hammer to identify its out-of-plane eigenfrequencies. Based on phase-sensitive optical reflectometry in the frequency domain, the measure of the phase along the fiber provides the spatial and temporal distribution of the mechanical deformation inside the coil.

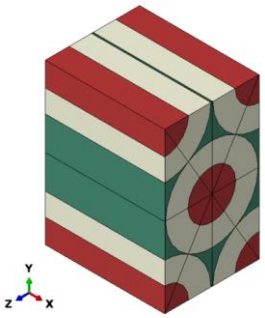

Figure 1: Representative volume element (RVE) selected for the actual coil case [2]

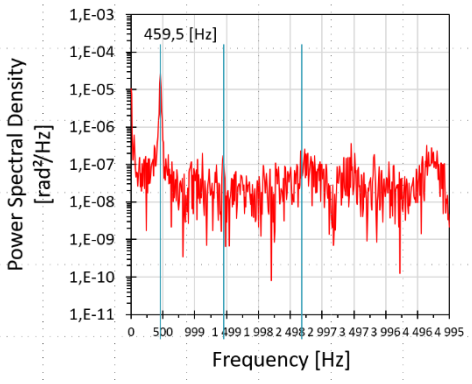

Figure 2: Frequency plot of the orthoradial modes using an optical interrogator

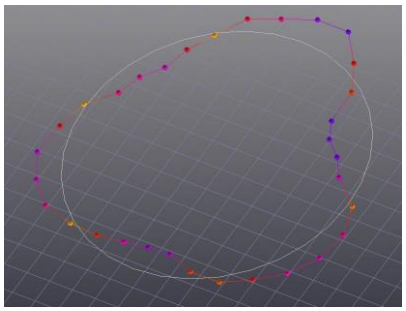

Figure 3: 2nd radial mode (shock hammer, LMS)

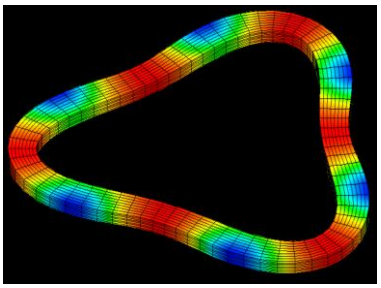

Figure 4: 2nd radial mode (Cast3M)

Validation of numerical and experimental results

At a given position in the fiber, a frequency plot derived from OFDR (Optical Frequency Domain Reflectometry) measurements was performed (figure 2). On the spectrum of this trace, we observe an amplitude peak at 459 Hz, corresponding to one of the resonance modes of the coil. The other frequencies, 1452 and 2622 Hz, are not as clearly visible, perhaps due to an averaging effect related to the spatial resolution (1 measurement point taken per perimeter of the coil). The eigenfrequency values from the optical interrogator are therefore reliable and consistent with the experimental results, with a relative deviation of 0.74, 1.18 and 2.53% respectively for the first 3 off-plan modes.

REFERENCES

[1] I. A. ESIPENKO, D. A. LYKOV, AND O. Y. SMETANNIKOV, Using the transversely isotropic characteristics of the coil to calculate the thermal-drift parameters of a fiber-optic gyroscope, Opticheskiı Zhurnal 86, 36–44, May 2019.

[2] Özkan Kahveci, Caner Gençoglu and Tuncay Yalçinkaya, Experimental Analysis and Multiscale Modeling of the Dynamics of a Fiber-Optic Coil, Paulo Caldas, 2022.

[3] Pierre Travers, De la sensibilité accélérométrique des oscillateurs optoélectroniques à la mesure dynamique de déformations dans les fibres optiques, 2023.

[4] P. Travers , G. Arpison , I. Ghorbel, Y. Léguillon , F. Louf, P-A. Boucard, V. Kemlin, and V. Crozatier, Distributed Strain Sensing Inside a Fiber Coil Under Vibration, JOURNAL OF LIGHTWAVE TECHNOLOGY, VOL. 40, NO. 18, SEPTEMBER 15, 2022.

Integrating the role of dynamics in the crack propagation response of bonded structures

G. Ravanas , H. Bouvet , F. Daghia

TER M1 2022-2023
Final defence of research projects

école normale supérieure paris–saclay

TER M1 2022-2023
FINAL DEFENCE OF RESEARCH PROJECTS
April 18, 2023, Gif-sur-Yvette, France

Integrating the role of dynamics in the crack propagation response of bonded structures

G. Ravanas*, H. Bouvet*, F. Daghia†

* Département de Génie Mécanique
Université Paris-Saclay, ENS Paris-Saclay
91190 Gif-sur-Yvette, France
e-mail: gaston.ravanas@ens-paris-saclay.fr / hippolyte.bouvet@ens-paris-saclay.fr

† Laboratoire de Mécanique Paris-Saclay
Université Paris-Saclay, CentraleSupélec, ENS Paris-Saclay, CNRS, LMPS
91190, Gif-sur-Yvette, France
e-mail: federica.daghia@ens-paris-saclay.fr

KEYWORDS: fracture mechanics; composite materials; bonded structures; dynamic crack propagation; spring-mass systems.

ABSTRACT

General context

Composite materials have largely drawn the attention of the aerospace industry thanks to their advantageous ratio between low weight and high mechanical proprieties. The study of the crack propagation response in bonded structures is however still an active field of research. While bolted and riveted assemblies have traditionally been used for their reliability, they account substantially for local stress concentration as well as the overall weight and manufacturing time of an aircraft.

Several promising solutions involving the addition of stop holes and wire mesh along the bondline [1] or laser-based surface treatments allowing fibers to be used as crack-bridging ligaments [2] have experimentally demonstrated an improvement in the mechanical response and a general increase in mode I fracture toughness. Recent work by [3] has also brought attention to the use of widely different macroscopic cohesive length to allow for gradual dissipation mechanisms without decreasing the damage threshold. These cohesive lengths could be obtained with crack-bridging ligaments of different mechanical proprieties along the Cohesive Zone (CZ).

If previous studies have focused, often exclusively, on quasi-static responses, little attention has been paid to the dynamic response of bonded structures that could lead to harmful chain reactions during the fracture process. The aim of this supervised research project was therefore to understand and identify conditions leading to dynamic amplification that could further weaken the structural integrity of such bonded structures. This was achieved first through the discrete study of failing spring-mass systems during quasi-static loading. Second, through a continuous study employing a Finite Element Method (FEM) model of Double Cantilever Beam (DCB) sample embedded with crack-bridging ligaments under mode I loading.

Spring-mass system analysis

In order to make sense of the dynamic processes occurring during quasi-static loading, one needs to understand the aftermath of the first failing bridging ligament. The crack planes and ligaments can be modeled in a first approximation as masses m_i in series associated with springs k_{ij} in

parallel with a given elastic limit x_{ij} under loading $\bar{u}(t)$ as shown in Fig. 1. Studying the dynamic behavior of canonical spring-mass systems with one or more degrees of freedom (dof), *i.e.* two or more masses in series as the last one is displacement-dependent, with a given breaking spring allows one to extrapolate patterns of behavior in a more generic context.

A program has thus been developed in MATLAB to simulate any spring-mass architecture derived from Fig. 1 and study the dynamical response of various spring, elastic limit and mass distribution of a fixed-energy system after first failure. In a one dof system, results show that further spring failure is independent from mass distribution and that it is entirely dependent on quasi-static considerations. For systems with a higher number of dofs, different modes are interfering and local stress concentration can lead to unexpected spring failure following complex mass and spring-dependent patterns.

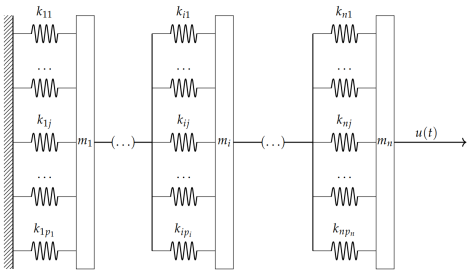

Figure 1: Generic spring-mass system

FEM simulation

In order to simulate the response of the bonded structure under mode I loading, several 2D FEM calculations were conducted in Abaqus. The first model was a beam composed of an elastic material and a CZ subjected to tension until the CZ failed. This model made it possible to highlight the phenomenon of stress propagation in the direction of the beam as well as the overshoot phenomenon. Indeed, a stress higher than the stress before failure was observed. In order to approximate the real case, force and displacement calculations of a classical DCB model with a cohesive zone at the level of the crack were carried out in static and dynamic mode. The models showed similar behavior for low speeds. Finally, a small area of the cohesive zone was removed in order to replace it with a cohesive zone with a higher fracture toughness. The aim was to get closer to the DCB configuration which models bridging ligaments with bi-linear springs. The simulation showed, as expected, a rebound in the force versus displacement curve.

Further work

A better understanding of the complex mechanisms taking place in higher number of dofs and larger spring-mass systems is still required to be able to generalize dynamical behavior after first failure. Furthermore, in order to observe the rupture of the cohesive element modeling the bridging ligament in the FEM simulation, a model with two parallel cohesive zones is required.

REFERENCES

[1] K. Maloney, N. Fleck. Toughening strategies in adhesive joints. *International Journal of Solids and Structures* **158**: 66-75, 2019.

[2] R. Tao, X. Li, A. Yudhanto, M. Alfano, G. Lubineau. Laser-based interfacial patterning enables toughening of CFRP/epoxy joints through bridging of adhesive ligaments. *Composites Part A: Applied Science and Manufacturing* **139**: 106094, 2020.

[3] F. Daghia, V. Fouquet, L. Mabileau. Improving the crack propagation response of layered and bonded structures through dissipation mechanisms at different length scales. *International Journal of Solids and Structures* **254-255**: 111910, 2022.

Tomographic and numerical monitoring of a cracking test on ABS obtained by additive manufacturing

B. Fournier , A. Pillet , B. Smaniotto, F. Hild

TER M1 2022-2023
Final defence of research projects

école normale supérieure paris-saclay

TER M1 2022-2023
FINAL DEFENSE OF RESEARCH PROJECTS
March xx, 2023, Gif-sur-Yvette, France

Tomographic and numerical monitoring of a cracking test on ABS obtained by additive manufacturing

B. Fournier*, A. Pillet*, B. Smaniotto*,◇, F. Hild◇

École normale supérieure Paris-Saclay
4 Avenue des Sciences, 91190 Gif-sur-Yvette, France
* Department of Mechanical Engineering
e-mail:{bastien.fournier,aurelie.pillet}@ens-paris-saclay.fr
◇LMPS - Laboratoire de Mécanique Paris-Saclay
e-mail: {francois.hild,benjamin.smaniotto}@ens-paris-saclay.fr

KEYWORDS: Digital Volume Correlation; Cracking Test; Stress Intensity Factor; Energy Release Rate; Tomography.

ABSTRACT

Objects made of ABS obtained by additive manufacturing are mostly fabricated by fused deposition modeling. Yet, the fracture properties of this material have been rarely reported. This project aims at performing an in situ cracking test to obtain tomographic scans. The reconstructed volumes were analysed with digital volume correlation to measure displacement fields. The main purpose of this project was to determine stress intensity factors and energy release rate for the whole experiment.

Methods A cracking test was monitored using micro-computed tomography (Figure 1(a)). This imaging technique is non-destructive and gives access to 3D images of the sample. The two grips were made of ABS and designed with Catia modeler. Their relative motion was controlled during the in situ test. Two scans in the reference configuration were aquired in order to assess the mesurement uncertainties. Then, eight scans were performed with different levels of applied displacements until reaching 3 mm (Figure 1(b)). Finally, the applied displacement was decreased to return to the initial position of the grips.

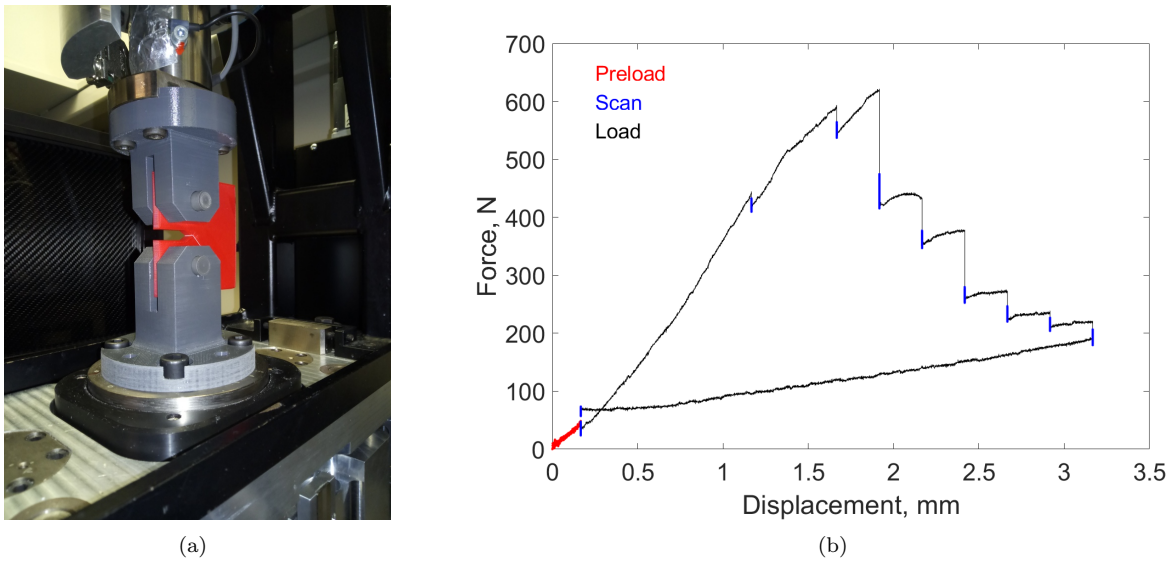

(a) (b)

Figure 1: (a) In situ cracking test. (b) Corresponding force displacement curve.

The compact tension sample had a size of $74 \times 77 \times 6.1$ mm^3 with a 74.1 µm per voxel resolution. 3D images were reconstructed using the tomographic scans. Then, Digital Volume Correlation (DVC) was used in order to measure displacement fields. In the present case, a finite element implementation was used [1]. A first mesh with four noded tetrahedra was created. The crack path was then estimated from the gray level residuals of a first DVC analysis for which the presence of the crack was not accounted for. Then, the nodes were split along the crack path and a subsequent DVC analysis was conducted. Crack opening displacement (COD) fields were

measured. The normal to the crack path was calculated, and the CODs were then projected onto it (i.e., mode I component). A square root interpolation of the latter was made considering that before the crack front it was canceling out. The final crack front was chosen as the one that minimized the error between the interpolation and the measured mode I COD. This crack front will be then used in order to determine the stress intensity factors (SIFs) and the energy release rate using Williams' series. The latter correspond to the displacement solution of a cracked elastic medium [2]. Each elementary displacement field was then calculated over pac-man like meshes, which were placed on the estimated crack front position of each node layer of the sample mesh. The amplitudes associated with each elementary field were obtained via least squares fit between the Williams' series and the measured displacement fields. The SIFs for each mode are proportional to the amplitude of the one half Williams' fields.

Results

Figure 2(a) shows the displacement field of the sample for the last scan. A rather large amplitude of 70 voxels (or about 5 mm) is observed. The crack started to propagate perpendicular to the loading direction and then bifurcated along a 45° direction, which corresponds to one of the printing directions. The mode I COD field of scan 8 was significantly larger in amplitude in comparison to the other two fields. This result proves that the experiment was predominantly in mode I even though kinking occurred. Figure 2(b) diplays the mode I stress intensity (K_I) factors for the eight scans. This factor varies from 2.5 to 3.5 MPa$\sqrt{\text{m}}$ for the last six scans. There are in good agreement with litterature results [3] where the fracture toughness K_{Ic} varied from 3.2 to 3.8 MPa$\sqrt{\text{m}}$. K_I profile changes along the thickness direction, which shows the interest of performing 3D analyses thanks to in-situ tests and DVC. Last, the energy release rate varied from 4 to 9 kJm^{-2} during the post bifurcated propagation, which is also consistent with reported levels [3].

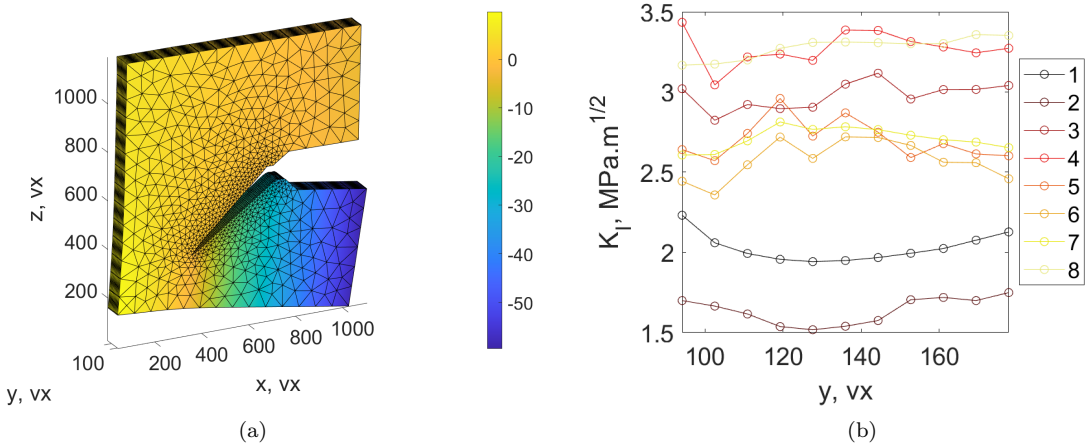

(a) (b)

Figure 2: (a) Measured vertical displacement field of scan 8 expressed in voxels shown on the deformed configuration (amplified 2 times). (b) Mode I stress intensity factor (K_I) profiles for the eight scans depending on the position y along the crack front.

References

[1] F. Hild, A. Bouterf, L. Chamoin, *et al.*, "Toward 4D Mechanical Correlation," *Advanced Modeling and Simulation in Engineering Sciences*, vol. 3, no. 1, pp. 1–26, 2016.

[2] M. L. Williams, "On the Stress Distribution at the Base of a Stationary Crack," *Journal of Applied Mechanics*, vol. 24, no. 1, pp. 109–114, Jun. 2021.

[3] J. Gardan, A. Makke, and N. Recho, "Improving the fracture toughness of 3D printed thermoplastic polymers by fused deposition modeling," *International Journal of Fracture*, vol. 210, no. 1, pp. 1–15, Mar. 2018.